**Supplementary material for the manuscript:**

# The link between organic aerosol mass loading and degree of oxygenation: An α-pinene photooxidation study

**L. Pfaffenberger, P. Barmet, J. G. Slowik, A. P. Praplan[+], J. Dommen, A. S. H. Prévôt and U. Baltensperger**

Laboratory of Atmospheric Chemistry, Paul Scherrer Institute, 5232 Villigen, Switzerland

[+]Now at: Department of Physics, University of Helsinki, Helsinki, Finland

Correspondence to: A. S. H. Prévôt (Andre.Prevot@psi.ch)

**Table S 1:** Overview of HONO input into the smog chamber before switching on the lights. The last column contains the ratio between HONO and α-pinene initial concentrations.

| Expt. No. | initial HONO ppbv (±10% instrument accuracy) | α-pinene ppbv | HONO / α-pinene |
|---|---|---|---|
| 1 | 1.6 | 7 | 0.2 |
| 2 | 4.9 | 14 | 0.4 |
| 3 | 1.0 | 20 | 0.05 |
| 4 | 1.0 | 22 | 0.05 |
| 7 | 1.9 | 45 | 0.04 |
| 8 | 2.8 | 46 | 0.06 |
| 9 | 5.1 | 50 | 0.1 |

**Table S 2:** Conditions of blank experiments B1-B5. The SMPS mass concentration is only given for blank experiments without seed. Detection limit is abbreviated with DL.

| Blank No. | Maximum Organic mass | RH | T | NO | $NO_2$ | radiation | added | | Previous |
|---|---|---|---|---|---|---|---|---|---|
| | $\mu g \cdot m^{-3}$ | av(sd) % | av(sd) °C | av(sd) ppb | av(sd) ppb | source | ppb | seed $\mu g \cdot m^{-3}$ | SC use |
| (B1) | SMPS: 0.03 (Suspended) AMS: below DL | Ca. 50* | Ca. 22* | 0.9(0.3) | no data | UV+Xe | - | - | moped emissions (up to 100 $\mu g \cdot m^{-3}$) |
| (B2) | SMPS: 0.16 (Suspended) AMS: below DL | 49(2) | 21.8(0.6) | 1.0(0.3) | Below det.lim. | UV+Xe | - | - | α-pin photooxid. (2 - 73 $\mu g/m^3$) moped emissions (up to 100 $\mu g \cdot m^{-3}$) |
| (B3) | AMS: 1.7 (Suspended) | 61(6)** | 25.2(1.4) | 3.3(0.6) | Below det.lim. | UV+Xe | HONO 10 | $(NH_4)_2SO_4$ (6.6±0.2) | α-pin photooxid. (1.4 - 80 $\mu g \cdot m^{-3}$) |
| (B4) | AMS: 0.16 (wlc) | 80-85 | | | | UV+Xe | NO 40*** | $(NH_4)_2SO_4$ (1.8) | α-pin photooxid. (1.4 - 80 $\mu g \cdot m^{-3}$) |
| (B5) | AMS: 0.11 (wlc) | 80-85 | | | | UV+Xe | HONO ~2 | $(NH_4)_2SO_4$ (1.2) | α-pin photooxid. (1.4 - 80 $\mu g \cdot m^{-3}$) |

* During blank experiment B1, no radiation shielded *T*/RH measurement existed. 55 % RH and 19.5°C were measured in darkness before lights were switched on. Assuming the temperature increases by 3°C after lights are switched on, leads to a RH of 50 %.

** Before lights were switched on, 85 % RH and 19.2°C were measured. After lights were switched on, the temperature increased to 25°C, resulting in a decreased RH of 60.9 %.

*** 40 ppbv of NO added to the blank before lights were switched on.

29

30 **Table S 3:** Changes in unit mass resolution fragmentation table compared to Aiken et al.
31 (2008).
32

| m/z | Expt. 7 (with $NH_4HSO_4$ seed) | Expt. 1-6; 8-9 (without $NH_4HSO_4$ seed) | Aiken et al. (2008) (standard fragmentation table) |
|---|---|---|---|
| | **Organics** | | |
| 14 | 3.84·frag_organic[13] | (0.14-4.17)·frag_organic[13] | |
| 16 | 0.107·frag_organic[17] | 0.107·frag_organic[17] | 0.25·frag_organic[17] |
| 28 | 0.93·frag_organic[44] | 0.93·frag_organic[44] | 1·frag_organic[44] |
| 30 | 0.16·frag_organic[29] | 0.16·frag_organic[29] | 0.022·frag_organic[29] |
| 36 | 36,-frag_air[36] | 36,-frag_air[36] | |
| 37 | 37 | 37 | 37,-frag_chloride[37] |
| 38 | 38,-frag_air[38] | 38,-frag_air[38] | 38,-frag_chloride[38],-frag_air[38] |
| 39 | 5·frag_organic[38] | 5·frag_organic[38] | |
| 40 | 40,-frag_air[40] | 40,-frag_air[40] | |
| 46 | 0.025·frag_organic[44] | 0.025·frag_organic[44] | |
| 47 | 47 | 47 | |
| 48 | 4·frag_organic[62] | 0.19·frag_organic[62] | 0.5·frag_organic[62] |
| 64 | 0.35·frag_organic[50]+0·frag_organic[78] | 0.07·frag_organic[50]+0.03·frag_organic[78] | 0.5·frag_organic[50]+0.5·frag_organic[78] |
| 65 | 0.55·frag_organic[51]+0.15·frag_organic[79] | 0.55·frag_organic[51]+0.1·frag_organic[79] | 0.5·frag_organic[51]+0.5·frag_organic[79] |
| 80 | 2·frag_organic[94] | 1.1·frag_organic[94] | 0.75·frag_organic[94] |
| 81 | 0.4·frag_organic[67]+0.25·frag_organic[95] | 0.3·frag_organic[67]+0.35·frag_organic[95] | 0.5·frag_organic[67]+0.5·frag_organic[95] |
| 98 | 0.65·frag_organic[84]+0.55·frag_organic[112] | 0.5·frag_organic[84]+0.7·frag_organic[112] | 0.5·frag_organic[84]+0.5·frag_organic[112] |
| | **air** | | |
| 14 | 14,-frag_nitrate[14],-frag_organic[14] | 14,-frag_nitrate[14],-frag_organic[14] | 14,-frag_nitrate[14] |
| | **$NH_4$** | | |
| 16 | 0.77·frag_NH4[17] | 0.77·frag_NH4[17] | 16,-frag_water[16],-frag_air[16],-frag_sulfate[16],-frag_organic[16] |
| | **$NO_3$** | | |
| 46 | 46,-frag_organic[46] | 46,-frag_organic[46] | 46 |
| | **K** | | |
| 39 | 39,-frag_organic[39] | 39,-frag_organic[39] | 39 |

## Correction for collection and transmission efficiency

The volumes derived from the two instruments SMPS and AMS were compared, applying the following densities in g/cm³ to the AMS species: $\sigma_{Org}$=1.4; $\sigma_{SO4}$=1.78; $\sigma_{NO3}$=1.72; $\sigma_{NH4}$=1.75; $\sigma_{Chl}$=1.4. The AMS data were corrected by applying the following correction factors (CF) to the organic mass concentration based on the ratio $volume_{SMPS}/volume_{AMS}$. Possible reasons for a disagreement between SMPS and AMS are given in brackets.

CF=2.7 for experiment 1 (volume weighted $d_m$ = 60-70nm)
CF=1.5 for experiment 2 (volume weighted $d_m$ = 70nm)
CF=(1.0-1.2) for experiments 3, 4, 5, 6, 8, 9 (volume weighted $d_m$=150-200nm)
CF=1.5 for experiment 7 (bouncing of sulfate)

For experiments 1 and 2, the volume weighted mean diameter is on the lower edge of the AMS measurement range and therefore the AMS samples significantly less than the SMPS. As all experiments except expt. 7 were nucleation experiments, the chemical composition is not expected to vary substantially as a function of diameter, relevant for expt. 1.

**Table S 4:** Slope of ΔO:C/Δ(OH exposure) for the period where aging dominates (see Fig. S 8) and the OH exposure required to increase O:C by 0.05.

| Expt. No. | ΔO:C/Δ(OH exposure) [$10^{-9}$·$cm^3$·$h^{-1}$] | ΔOH exposure/ΔO:C [$10^7$·$cm^{-3}$·h / 0.05] |
|---|---|---|
| 4 | 0.20 | 24.50 |
| 3 | 0.35 | 14.43 |
| 8 | 0.84 | 5.96 |
| 1 | 0.93 | 5.37 |
| 2 | 1.10 | 4.55 |
| 9 | 1.11 | 4.50 |
| 6 | 1.52 | 3.29 |
| 7 | 1.57 | 3.18 |
| 5 | 1.63 | 3.07 |

Contribution of blank experiment B3 to experiment 4

We used the mass spectra (MS) measured after the first, second and third seeding period during blank experiment B3, representing different aging times and thus chemical composition, as input for the statistical tool ME-2 (multi-linear engine: model by Paatero et al. (1999), analysis interface by Canonaco et al. (2013) to estimate its contribution to the total organic mass concentration. For the ME-2 runs, the blank experiment mass spectrum was fixed (a-value: 0) and two more free components were allowed (similar to the approach of Lanz et al. (Lanz et al., 2007) for ambient measurements). 120 iterations (40 for each blank experiment MS) of the model using different randomly distributed initial values resulted in an average contribution of the constrained blank MS between 6.6-9.9% in the first two hours up to 10-20% in the last three hours of experiment 4 with the lowest organic mass concentration. For the model runs, the *m/z* range of 12-250 was used. 5 out of 40 iterations resulted in the following time series and mass spectra. The spectrum of blank experiment B3 was fixed as factor 1, shown in Fig. 1a and b. Fig. 1a shows a representative time series of the three factors found for experiment 4. Factor 2 can be interpreted as early SOA product, while factor 3 represents the later SOA product. Figure 1b includes the mass spectra input (factor 1) and output from the ME-2 model runs.

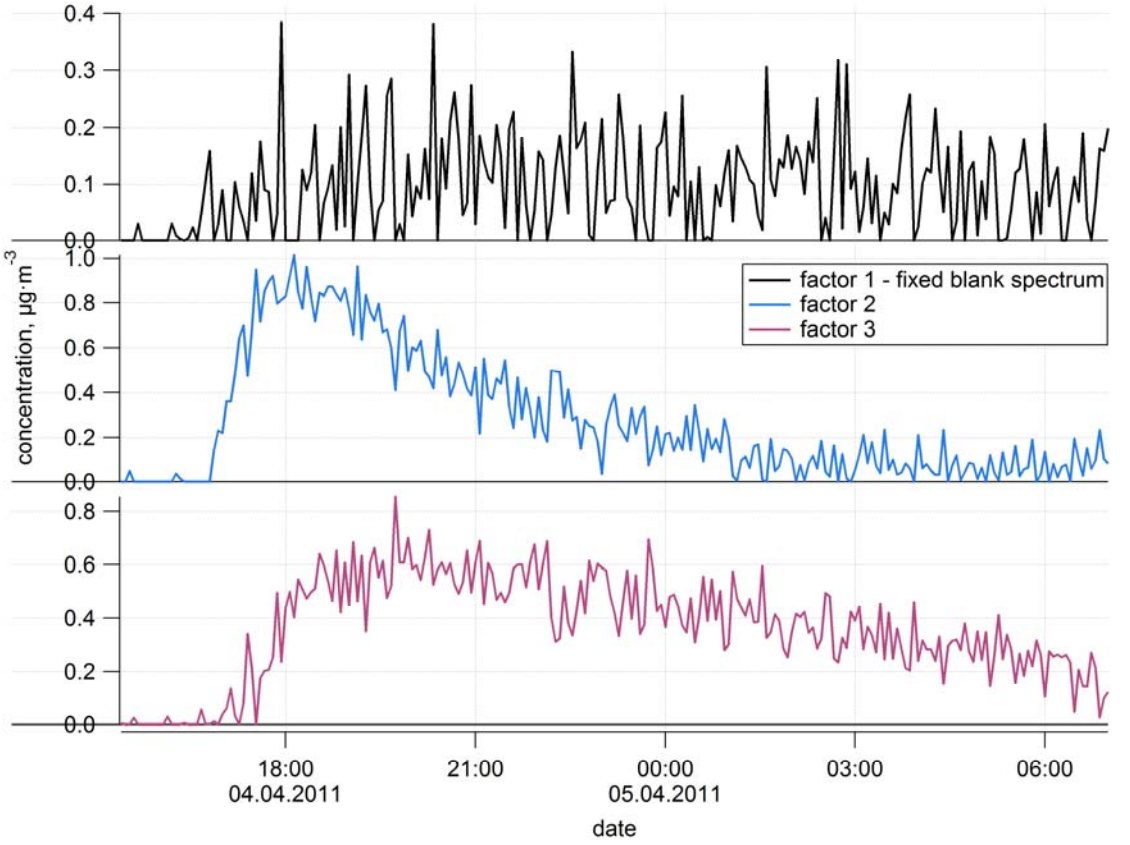


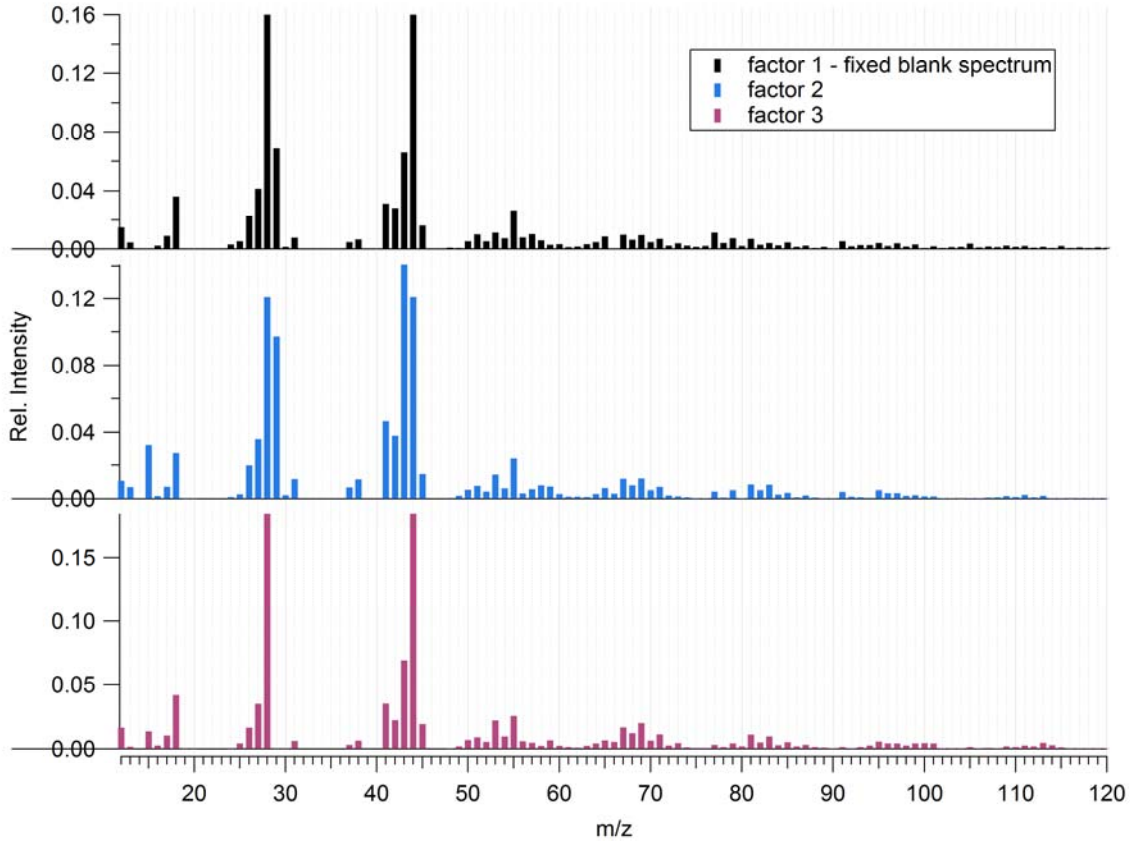


**Fig. S 1 a)** Time series of the concentration of the three factors (factor 1: fixed blank B3 spectrum, factor 2+3: two free spectra) and **b)** corresponding normalized mass spectra.

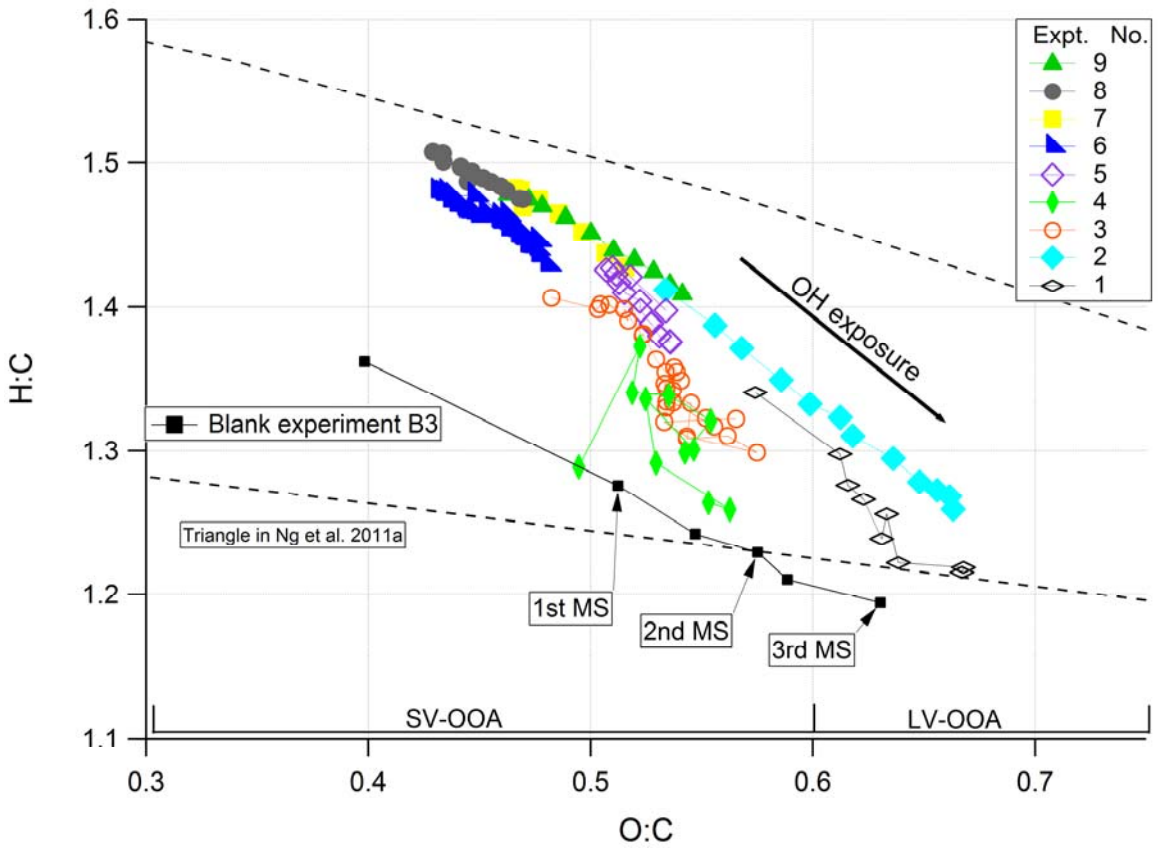


**Fig. S 2**: Van Krevelen diagram (H:C vs. O:C ratio) of the nine experiments together with the observed range of ambient SOA represented by dashed lines (Ng et al., 2011a) and blank experiment B3. Data points represent 30 min averages, except for Expt. 4 (60min average). Arrows indicate the time when mass spectra for ME-2 model runs were taken.

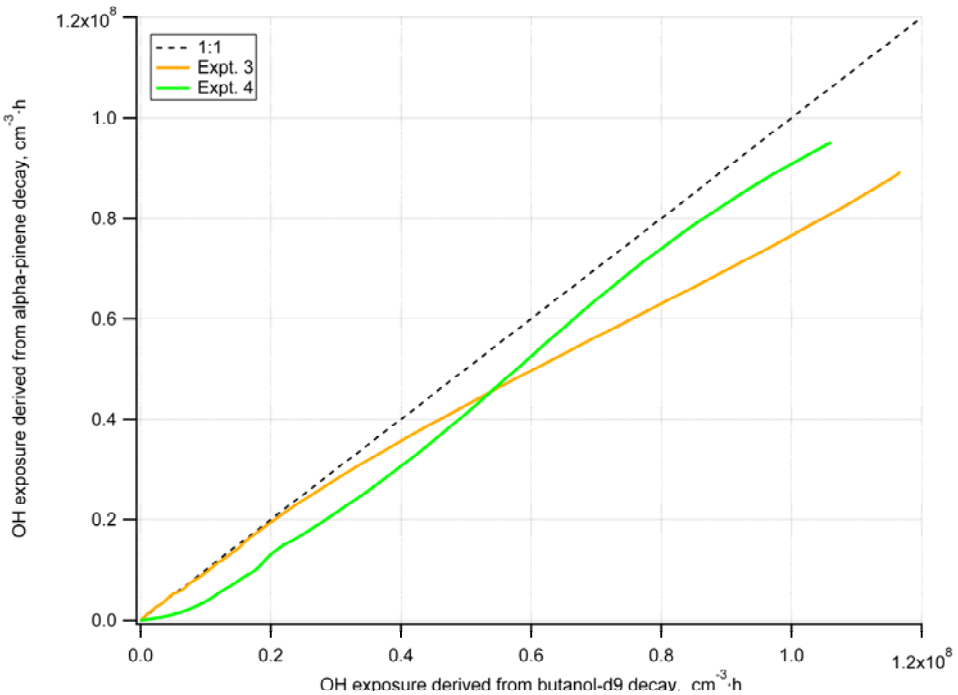


**Fig. S 3:** Comparison of OH exposures derived from α-pinene decay and butanol-d9 decay for experiments where butanol-d9 was above detection limit throughout the entire experiment. The dashed line represents the 1:1 line.

**Retrieval of the OH exposure of experiment 1 and 2 from a repeat experiment**

As the decay of α-pinene in the beginning of experiment 1 and 2 was very rapid, using the α-pinene method including the extrapolation to the whole experiment time leads to a possibly strong overestimation of the OH exposure. For this reason a repeat experiment was conducted which showed the same characteristics in α-pinene decay, but with the OH tracer butanol-d9 present for the whole experiment time (See Fig. S 4). The repeat experiment resembles strongly experiment 2, which has the same initial α-pinene concentration (14 ppbv). During experiment 1 (with an initial α-pinene concentration of 7 ppbv), the reactant decays within the same time. This lower initial α-pinene concentration is also the reason for the lower $O_3$ production. The replaced OH exposures derived from the α-pinene decay for experiments 1 (black line) and 2 (turquoise line) are shown in the lower panel together with the OH exposure of the repeat experiment (purple line).

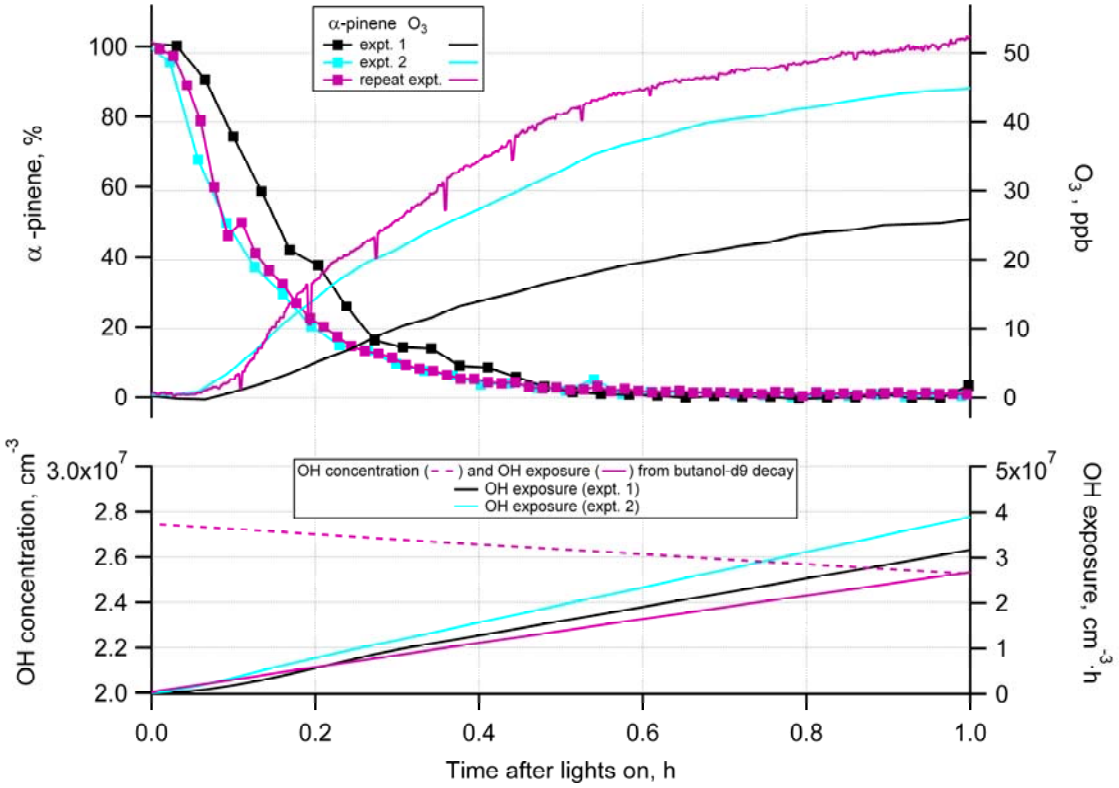


**Fig. S 4:** The α-pinene and $O_3$ concentrations of experiment 1, 2 and the repeat experiment are shown as a function of light exposure time (upper panel). The lower panel shows the OH concentration and exposure retrieved from the decay of the tracer butanol-d9, present during the repeat experiment as well as the OH exposures derived from the α-pinene method, which were replaced by the repeat experiment for analysis.

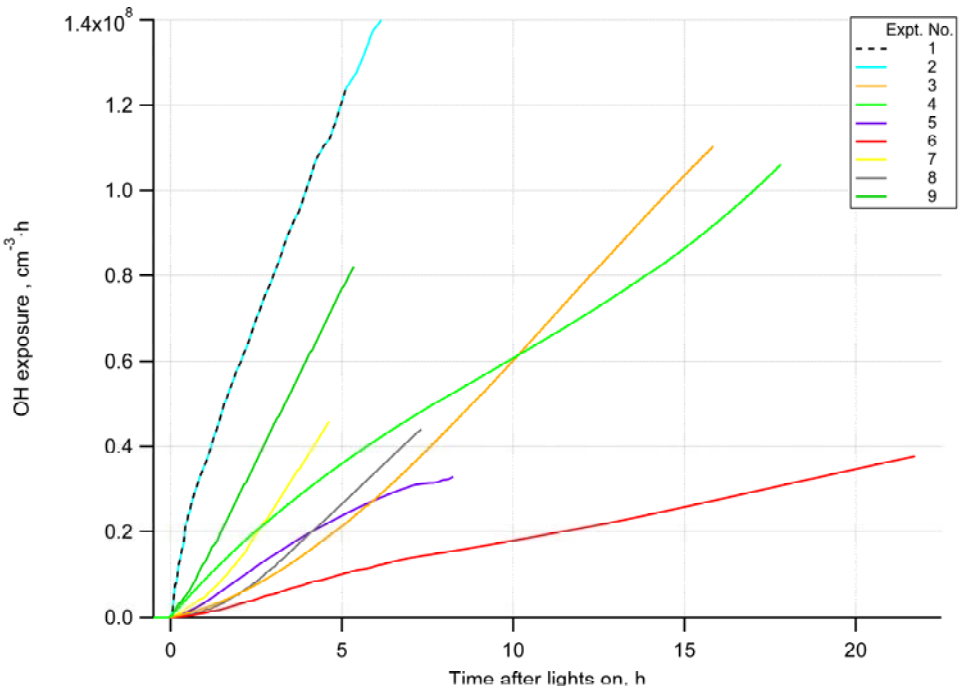


**Fig. S 5:** OH exposures for the nine different experiments (color code) derived from the decay of α-pinene, butanol-d9 or a combination of both. The OH exposure of experiment 1 and 2 was derived from a repeat experiment.

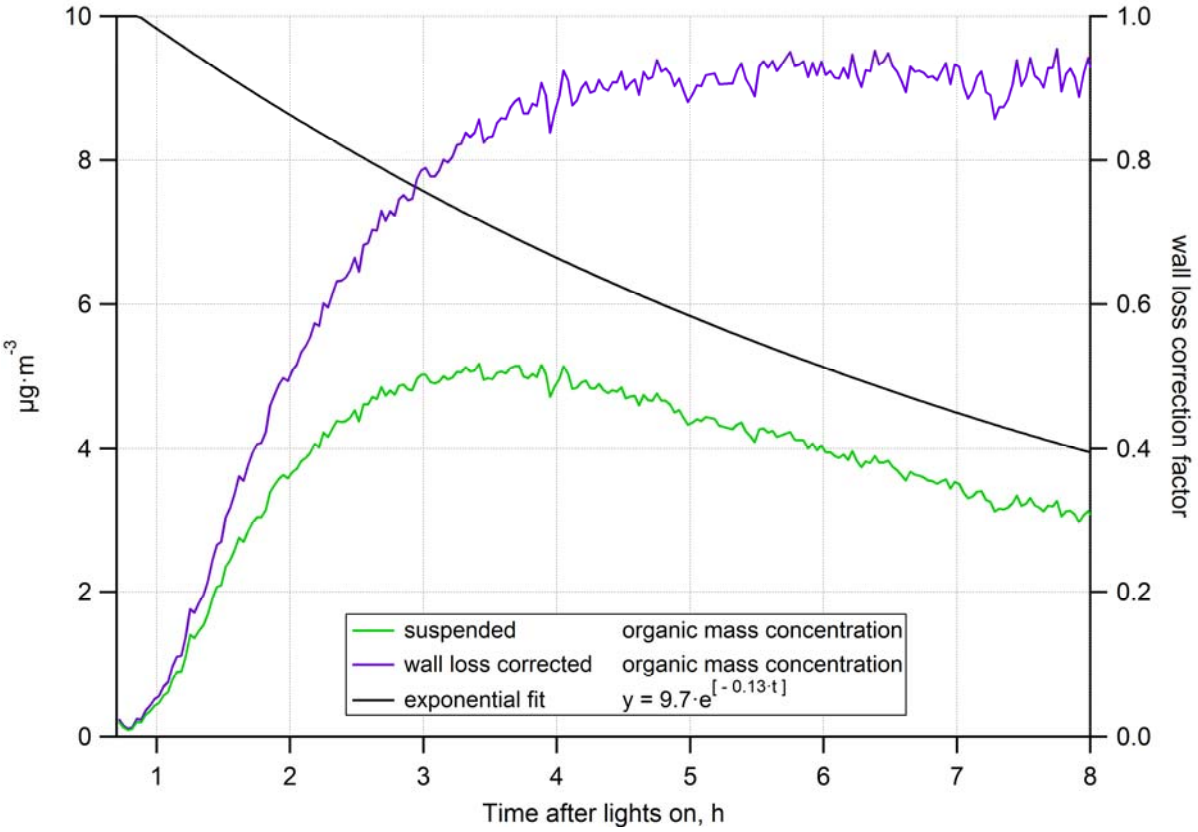


**Fig. S 6:** The measured organic mass concentration (green) was fitted exponentially (black) for the last three hours of experiment 5 where wall loss dominates over organic mass production. This procedure results in a lower limit of the wall loss corrected organic mass concentration (purple).

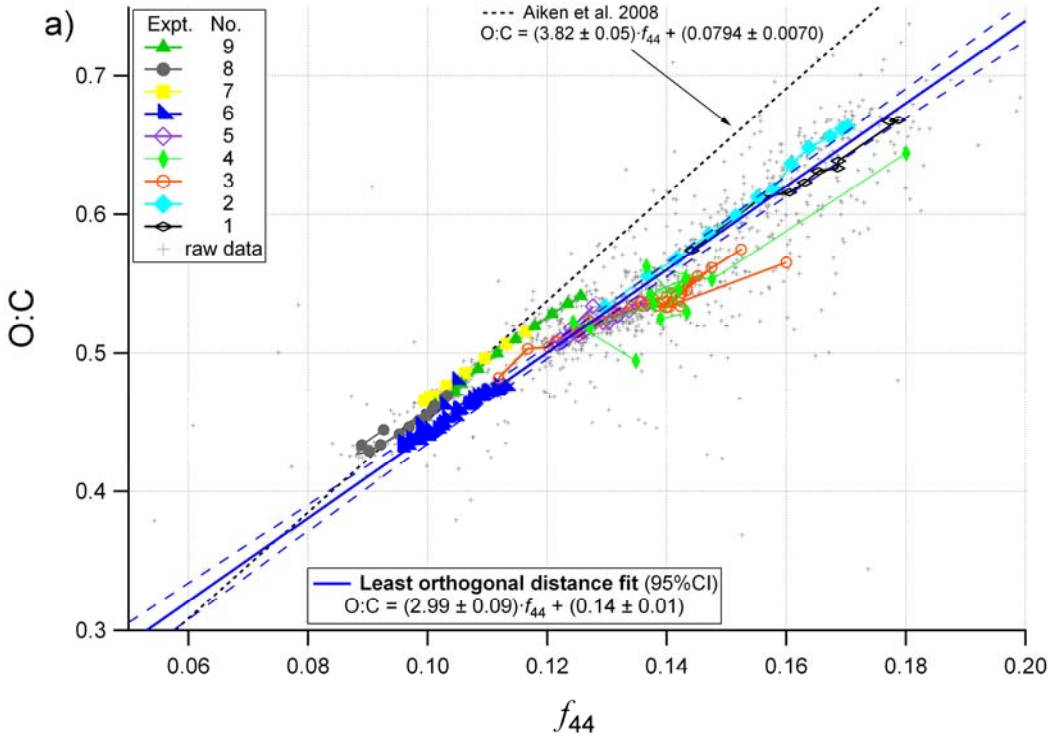


121

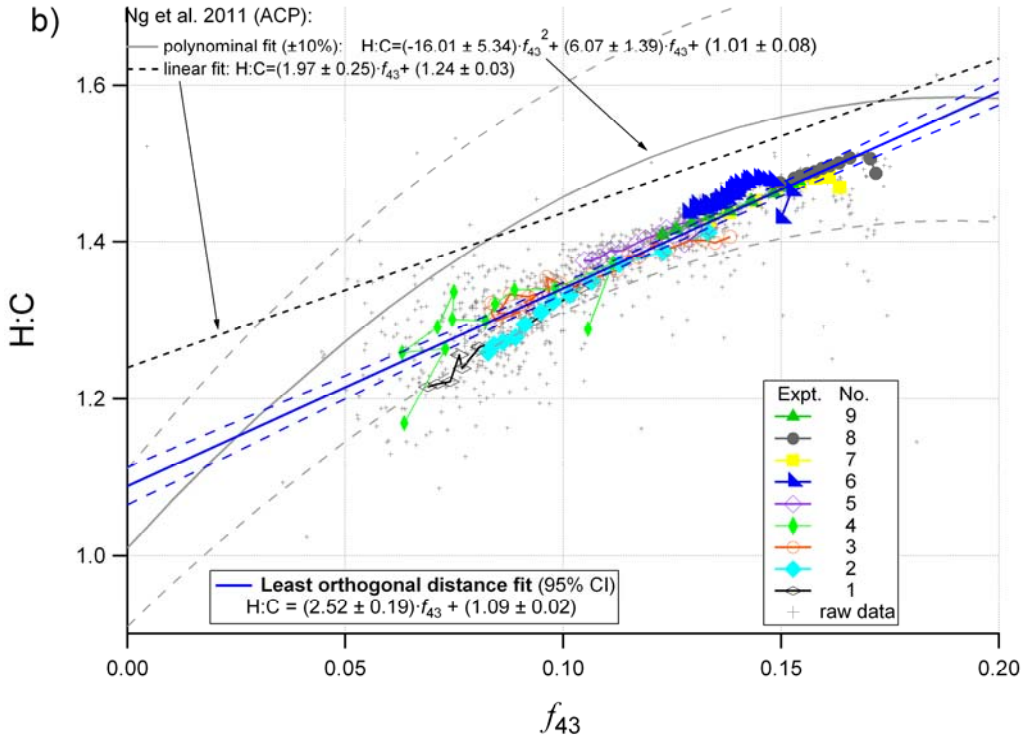


122

123 **Fig. S 7.** 30-min averages (except expt. 4: 60 min) of O:C ratio vs. organic mass fraction $f_{44}$
124 **(7a)** and of hydrogen-to-carbon ratio vs. organic mass fraction $f_{43}$ (**7b**) color coded for the
125 nine different experiments; 2-min data is represented by the grey dots. The linear regressions
126 are compared to the fit of Aiken et al. (2008) and to the linear and polynomial fit in Ng et al.
127 (2011a).

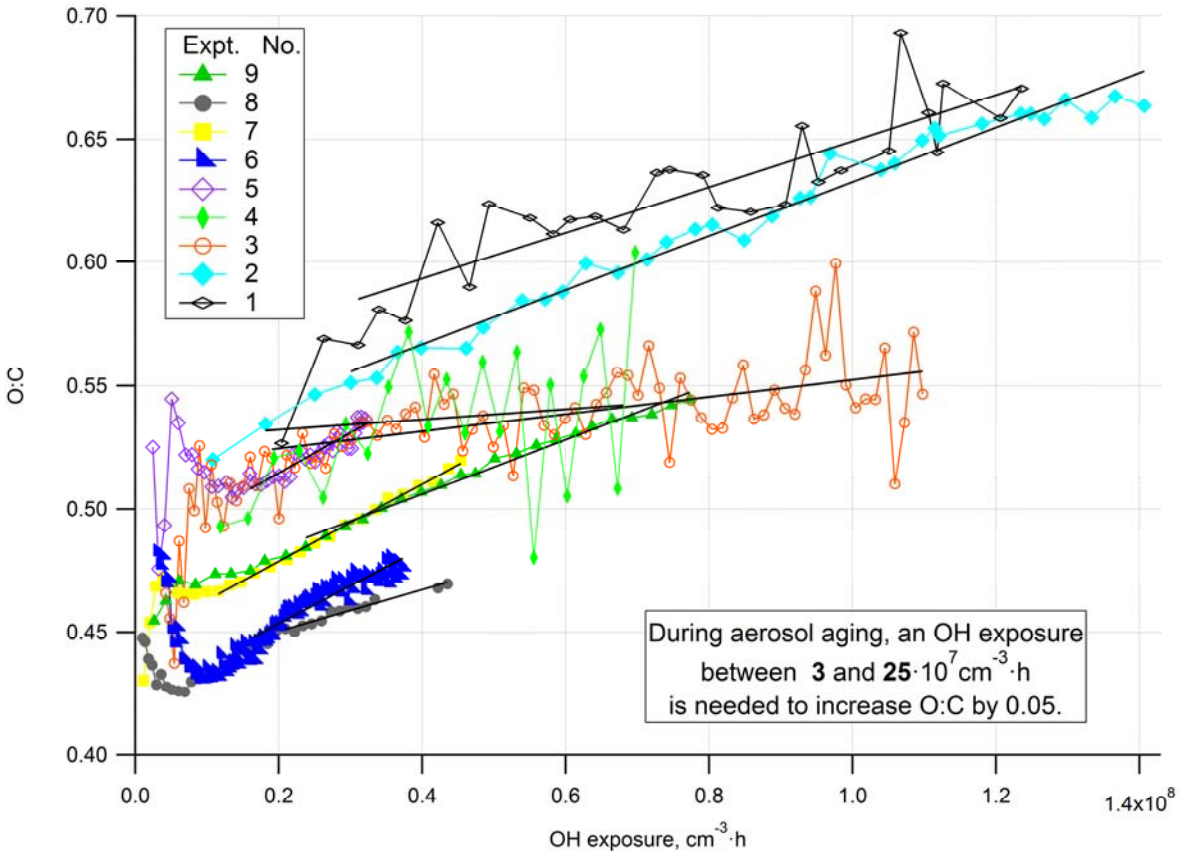


128

129

130 **Fig. S 8:** O:C ratio as a function of OH exposure for the nine smog chamber experiments.
131 The data was fitted with a line for the period when aging dominates, i.e. after the peak of
132 suspended organic mass is reached. The slopes of ΔO:C/Δ(OH exposure) are shown in Table
133 S4. An OH exposure between 3 and $25 \cdot 10^7$ $cm^{-3}$ ·h is required to increase O:C by 0.05.

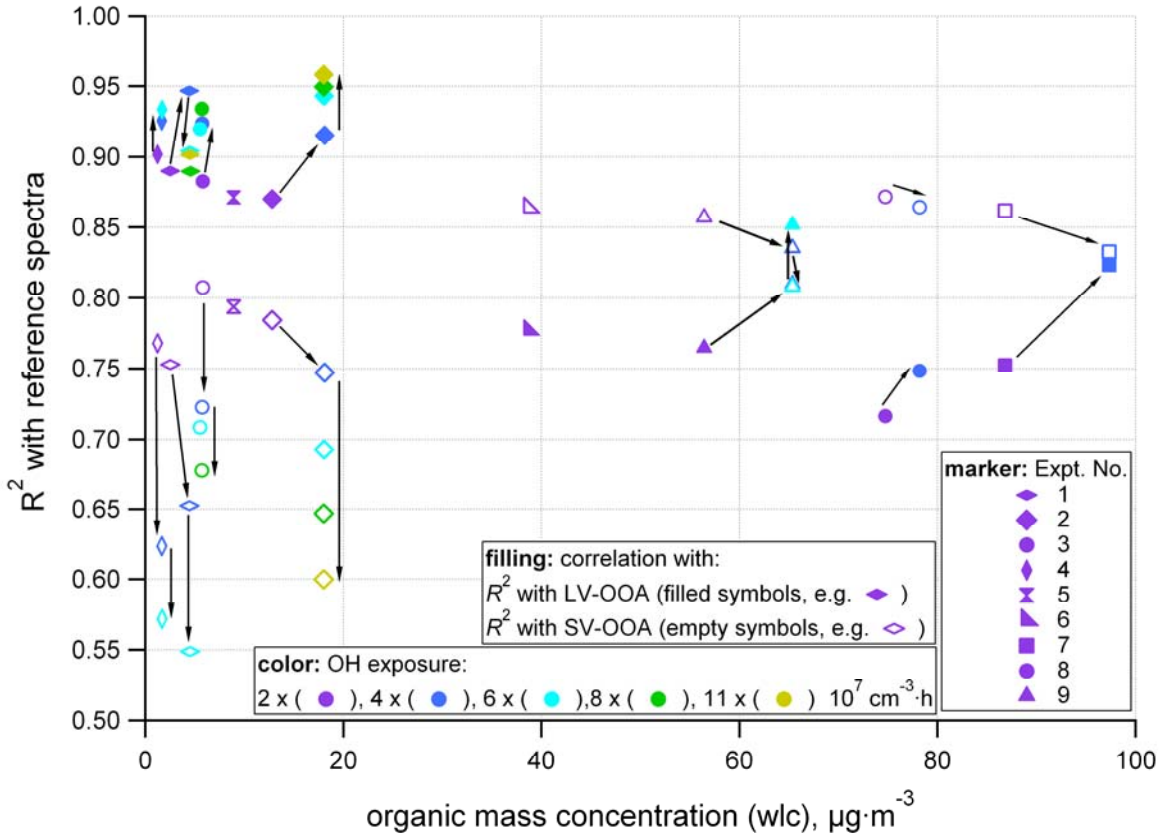


134

135

136 **Fig. S 9**: Squares of the Pearson correlation coefficients, $R^2$, of measured mass spectra in
137 comparison with LV-OOA (filled symbols) and SV-OOA (empty symbols) reference spectra
138 (Ng et al., 2011b) as a function of the organic mass concentration (wlc). The correlation was
139 performed on 30-min averaged MS at specific OH exposures (± 15 min) indicated by the
140 color code. The corresponding mass spectra are presented in Fig. S 10.

141

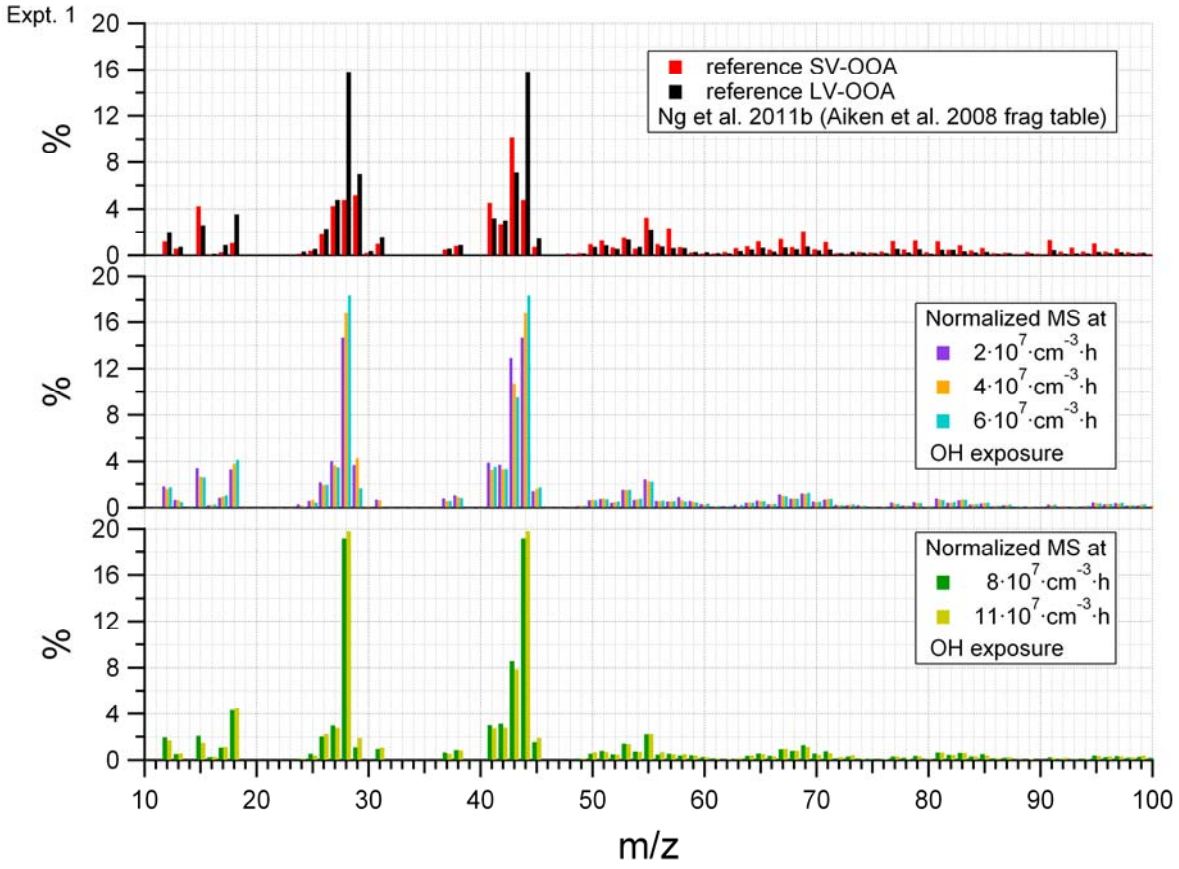
Expt. 1
reference SV-OOA
reference LV-OOA
Ng et al. 2011b (Aiken et al. 2008 frag table)
Normalized MS at
2·10^7·cm^-3·h
4·10^7·cm^-3·h
6·10^7·cm^-3·h
OH exposure
Normalized MS at
8·10^7·cm^-3·h
11·10^7·cm^-3·h
OH exposure
%
m/z

142

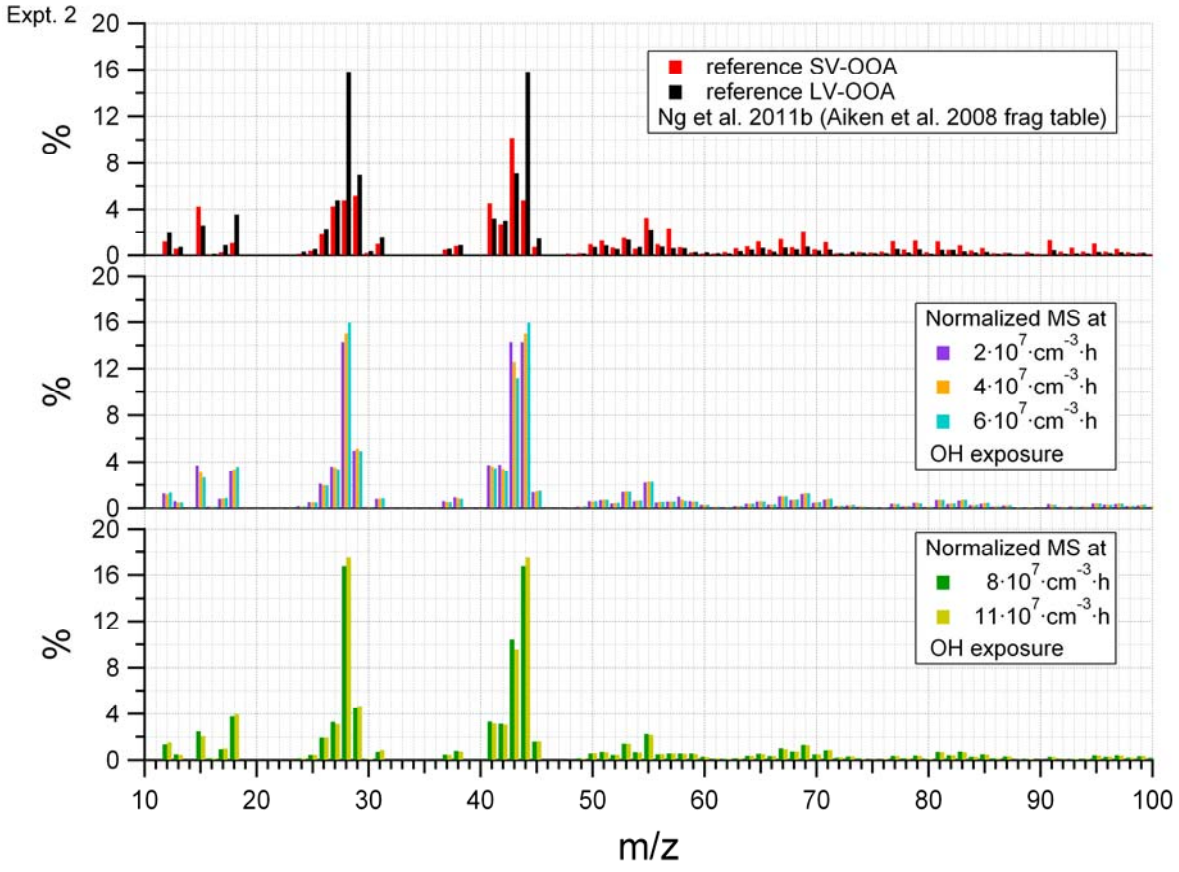
Expt. 2
reference SV-OOA
reference LV-OOA
Ng et al. 2011b (Aiken et al. 2008 frag table)
Normalized MS at
2·10^7·cm^-3·h
4·10^7·cm^-3·h
6·10^7·cm^-3·h
OH exposure
Normalized MS at
8·10^7·cm^-3·h
11·10^7·cm^-3·h
OH exposure
%
m/z

143

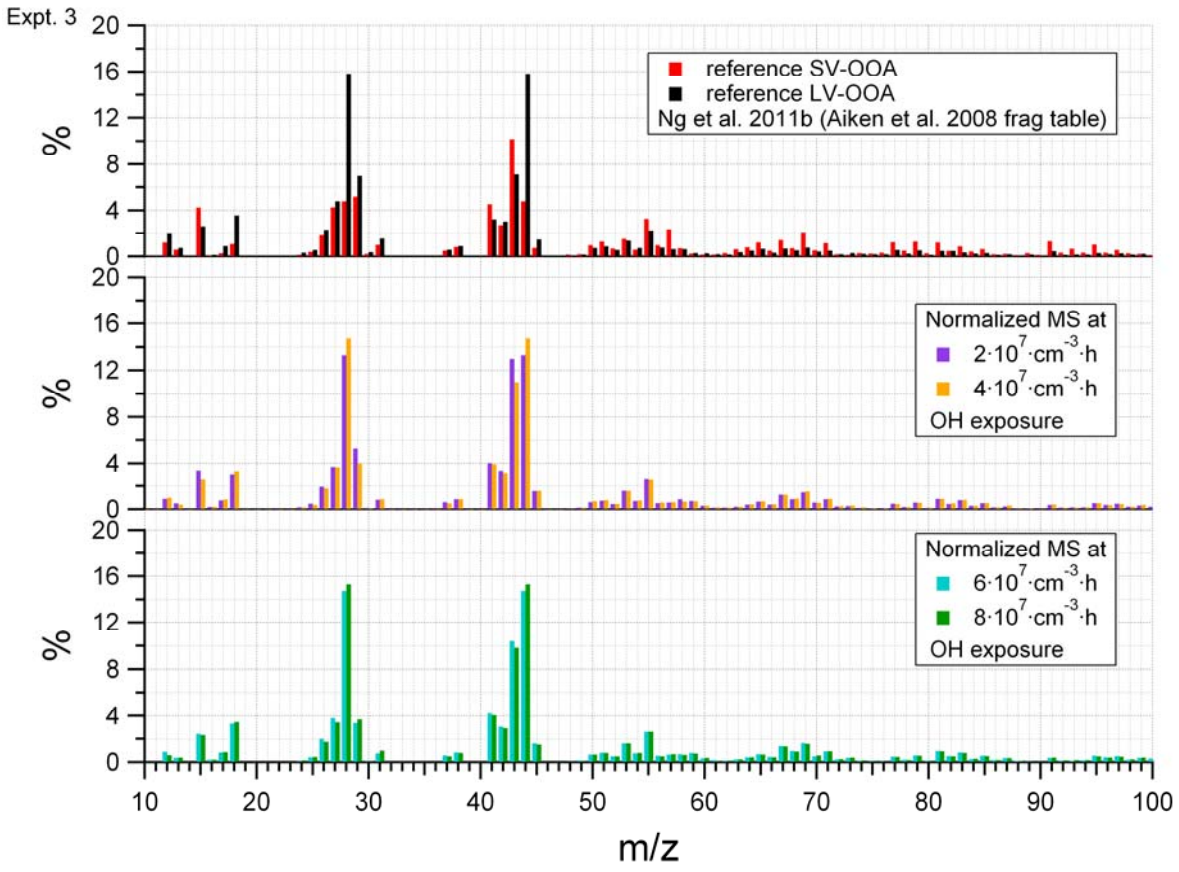
Expt. 3
reference SV-OOA
reference LV-OOA
Ng et al. 2011b (Aiken et al. 2008 frag table)
Normalized MS at
2·10^7·cm^-3·h
4·10^7·cm^-3·h
OH exposure
Normalized MS at
6·10^7·cm^-3·h
8·10^7·cm^-3·h
OH exposure
%
m/z

144

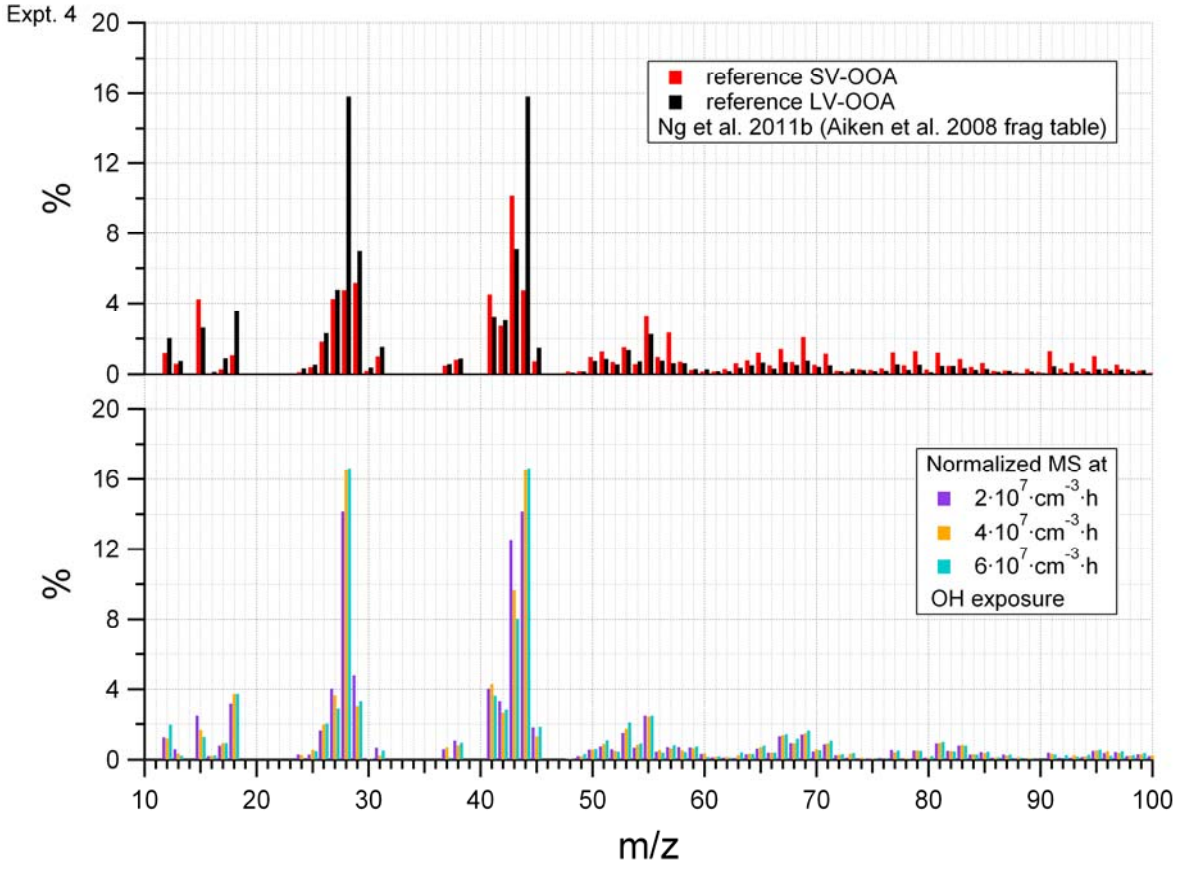
Expt. 4
reference SV-OOA
reference LV-OOA
Ng et al. 2011b (Aiken et al. 2008 frag table)
Normalized MS at
2·10^7·cm^-3·h
4·10^7·cm^-3·h
6·10^7·cm^-3·h
OH exposure
%
m/z

145

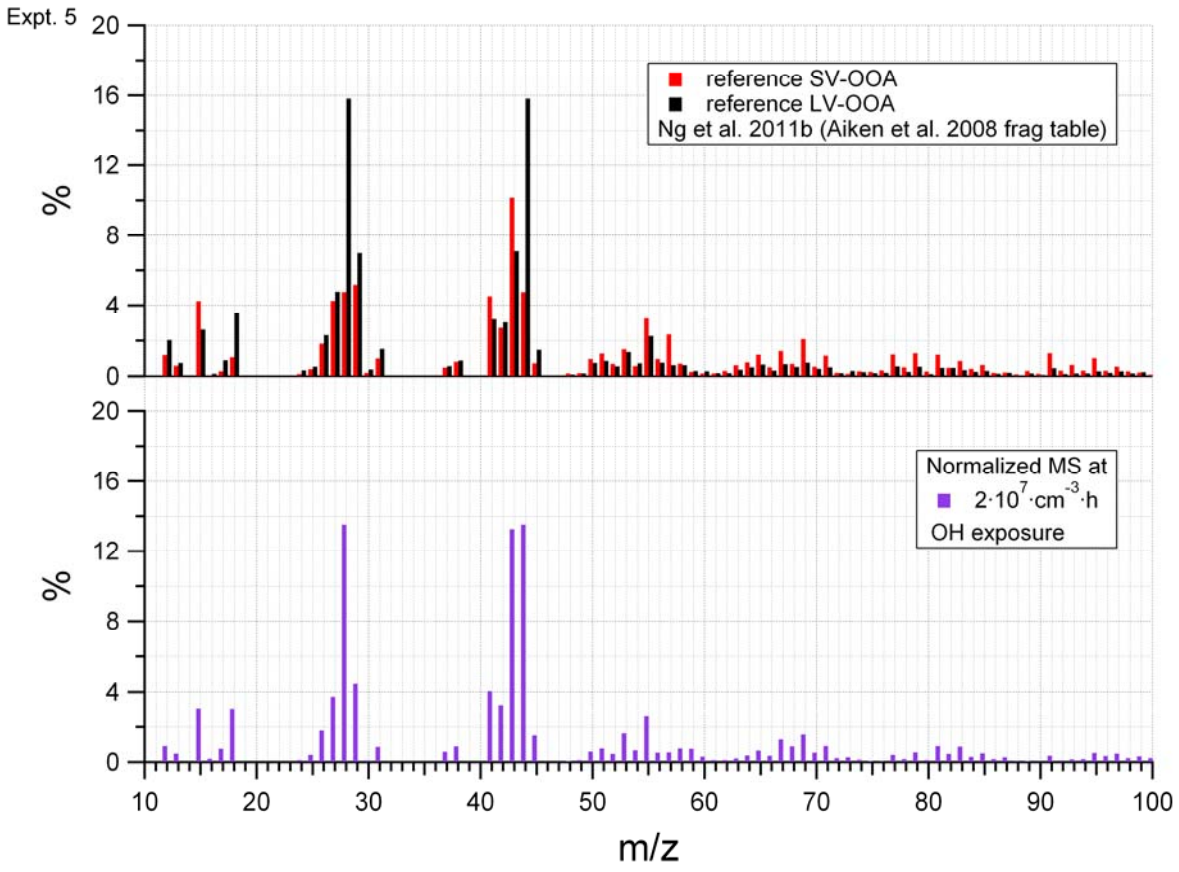
Expt. 5
reference SV-OOA
reference LV-OOA
Ng et al. 2011b (Aiken et al. 2008 frag table)
Normalized MS at
2·10^7·cm^-3·h
OH exposure
%
m/z

146

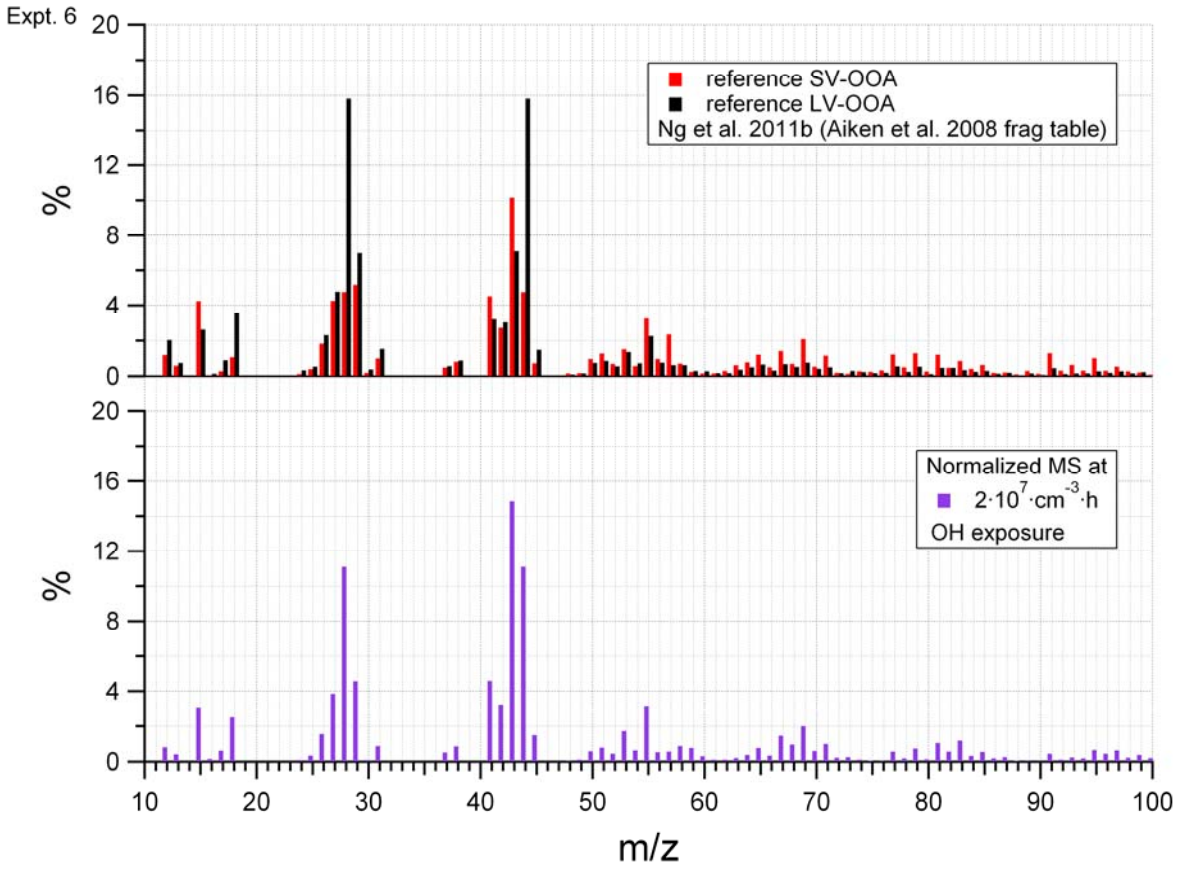
Expt. 6
reference SV-OOA
reference LV-OOA
Ng et al. 2011b (Aiken et al. 2008 frag table)
Normalized MS at
2·10^7·cm^-3·h
OH exposure
%
m/z

147

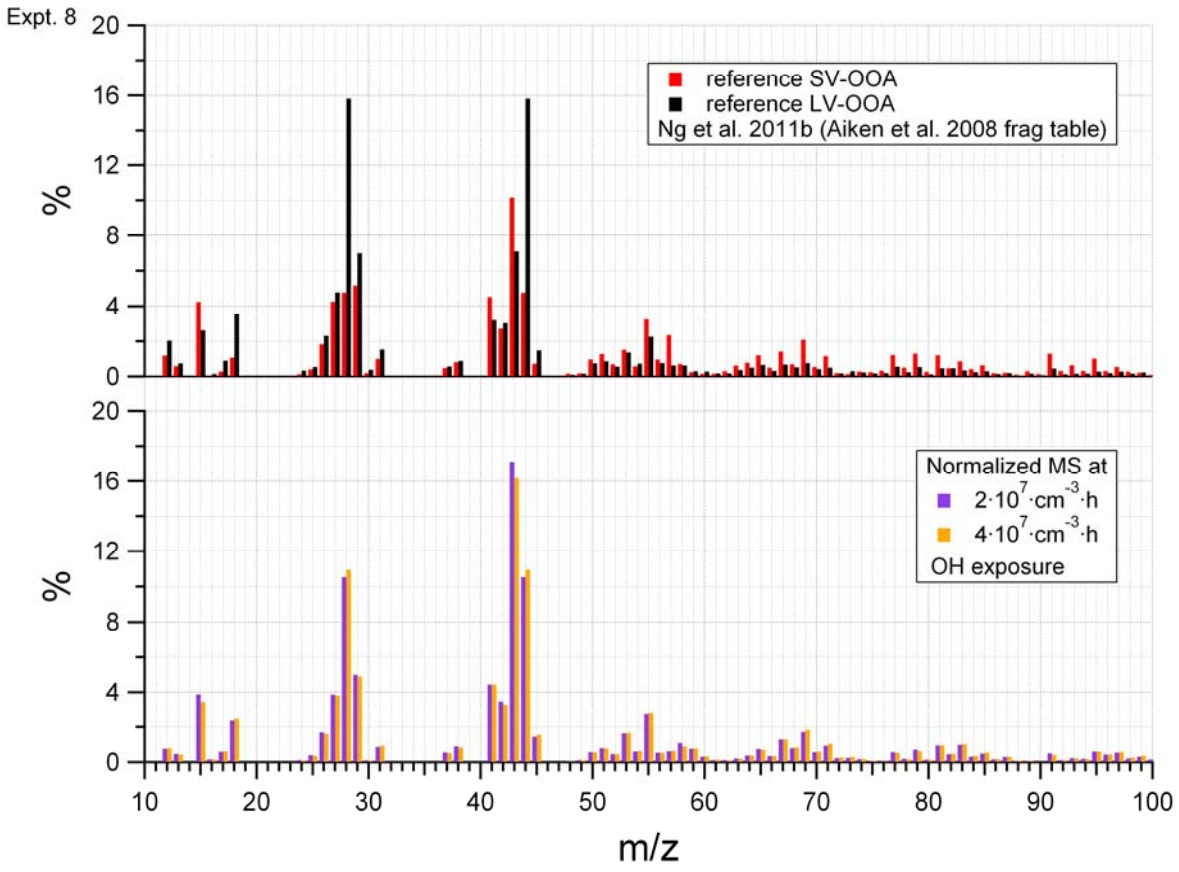
Expt. 8
reference SV-OOA
reference LV-OOA
Ng et al. 2011b (Aiken et al. 2008 frag table)
Normalized MS at
2·10^7·cm^-3·h
4·10^7·cm^-3·h
OH exposure
%
m/z

148

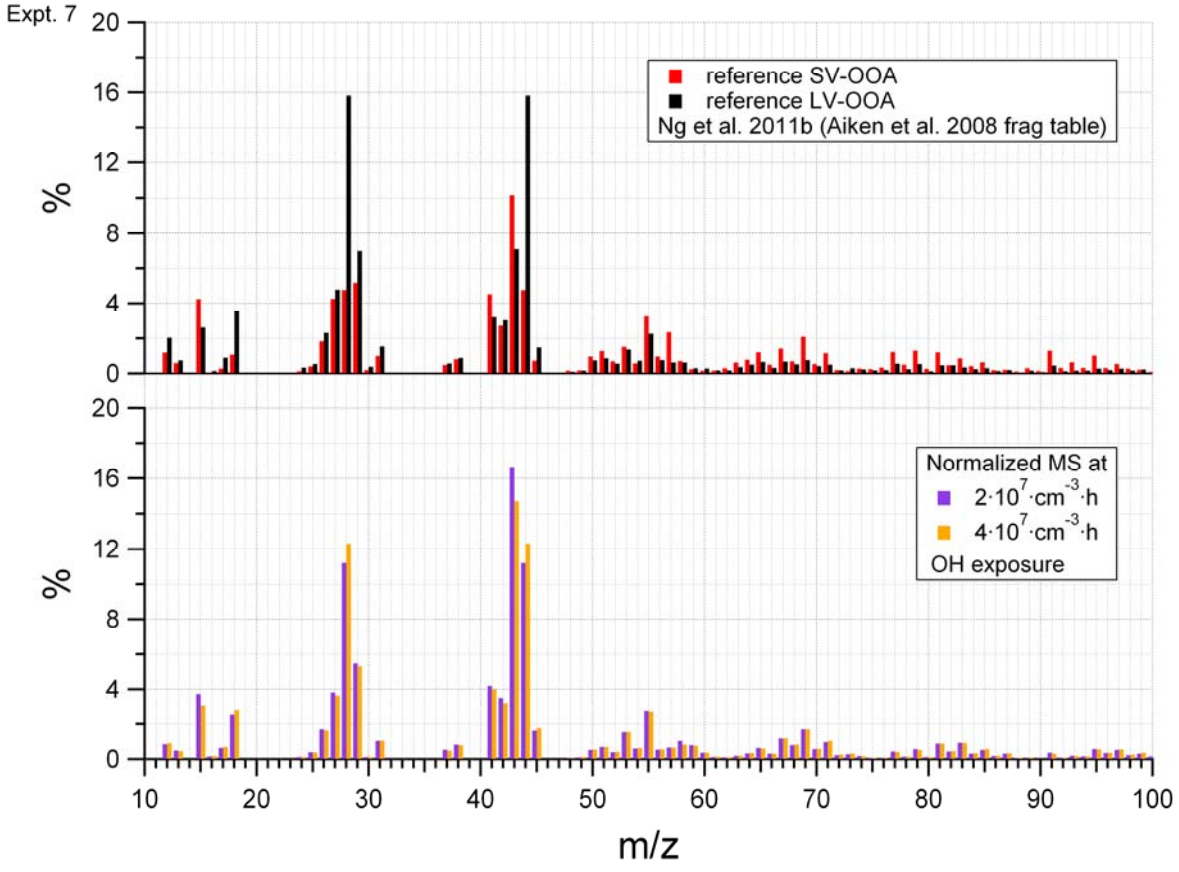
Expt. 7
reference SV-OOA
reference LV-OOA
Ng et al. 2011b (Aiken et al. 2008 frag table)
Normalized MS at
2·10^7·cm^-3·h
4·10^7·cm^-3·h
OH exposure
%
m/z

149

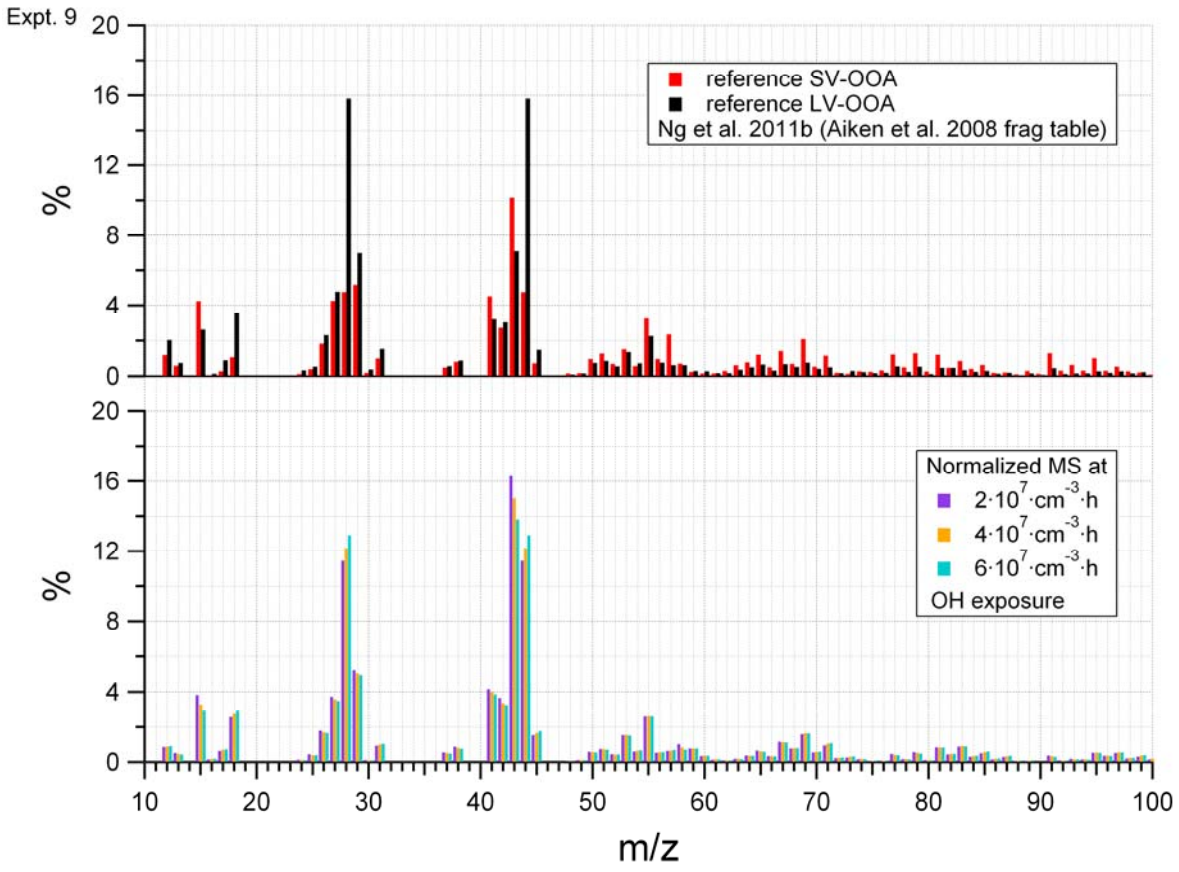


**Fig. S 10.** 30-min-averaged organic mass spectra of the nine experiments at OH exposures (if reached) of $2\cdot$, $4\cdot$, $6\cdot$, $8\cdot$, and $11\cdot10^7$ $cm^{-3}$ $\cdot h$ (±15 min), together with reference LV-OOA and SV-OOA spectra from Ng et al. (2011b). The reference spectra were converted to the fragmentation table of Aiken et al. (2008) and normalized. Correlation tests of each spectrum with both reference spectra were performed, while *m/z*'s directly proportional to *m/z* 44 and *m/z*'s present in only one, the measured or reference spectrum, were excluded.

158

159 **References**

160

161 Aiken, A. C., DeCarlo, P. F., Kroll, J. H., Worsnop, D. R., Huffman, J. A., Docherty, K. S.,
162 Ulbrich, I. M., Mohr, C., Kimmel, J. R., Sueper, D., Sun, Y., Zhang, Q., Trimborn, A.,
163 Northway, M., Ziemann, P. J., Canagaratna, M. R., Onasch, T. B., Alfarra, M. R.,
164 Prevot, A. S. H., Dommen, J., Duplissy, J., Metzger, A., Baltensperger, U., and
165 Jimenez, J. L.: O/C and OM/OC ratios of primary, secondary, and ambient organic
166 aerosols with high-resolution time-of-flight aerosol mass spectrometry, Environ. Sci.
167 Technol., 42, 4478-4485, 2008.
168 Canonaco, F., Crippa, M., Slowik, J., Baltensperger, U., and Prévôt, A. S. H.: A newly
169 developed interface for analyzing generalized Multilinear engine (ME-2) results:
170 Application on aerosol mass spectrometer data, in prep., 2013.
171 Lanz, V. A., Alfarra, M. R., Baltensperger, U., Buchmann, B., Hueglin, C., and Prevot, A. S.
172 H.: Source apportionment of submicron organic aerosols at an urban site by factor
173 analytical modelling of aerosol mass spectra, Atmos. Chem. Phys., 7, 1503-1522,
174 2007.
175 Ng, N. L., Canagaratna, M. R., Jimenez, J. L., Chhabra, P. S., Seinfeld, J. H., and Worsnop,
176 D. R.: Changes in organic aerosol composition with aging inferred from aerosol mass
177 spectra, Atmos. Chem. Phys., 11, 6465-6474, 2011a.
178 Ng, N. L., Canagaratna, M. R., Jimenez, J. L., Zhang, Q., Ulbrich, I. M., and Worsnop, D. R.:
179 Real-Time Methods for Estimating Organic Component Mass Concentrations from
180 Aerosol Mass Spectrometer Data, Environ. Sci. Technol., 45, 910-916, 2011b.
181 Paatero, P.: The multilinear engine - A table-driven, least squares program for solving
182 multilinear problems, including the n-way parallel factor analysis model, Journal of
183 Computational and Graphical Statistics, 8, 854-888, 10.2307/1390831, 1999.
184
185